# Local Fourier Analysis of Domain Decomposition and Multigrid Methods for High-Order Matrix-Free Finite Elements

Jeremy L Thompson

University of Colorado Boulder

*jeremy@jeremylt.org*

July 8, 2021

# Funding

This work is supported by the Exascale Computing Project (17-SC-20-SC), a collaborative effort of two U.S. Department of Energy organizations (Office of Science and the National Nuclear Security Administration) responsible for the planning and preparation of a capable exascale ecosystem, including software, applications, hardware, advanced system engineering and early testbed platforms, in support of the nation's exascale computing imperative.

# Overview

# Big Picture

- High-order matrix-free representations of PDEs are better suited to modern hardware than sparse matrices
- High-order matrix-free representations require preconditioned iterative solvers
- Local Fourier Analysis (LFA) provides sharp convergence estimates for these preconditioners
- We develop LFA of p-multigrid and Balancing Domain Decomposition by Constraints (BDDC) on high-order element subdomains
- Further, we investigate LFA of p-multigrid with a BDDC smoother

# Reproducibility

Transparency and reproducibility are the lifeblood of scientific advancement

All software and data used in this dissertation is all open source

- https://www.github.com/jeremylt/LFAToolkit.jl
- https://www.github.com/CEED/libCEED
- https://www.mcs.anl.gov/petsc
- https://github.com/jeremylt/dissertation

# Modern Hardware

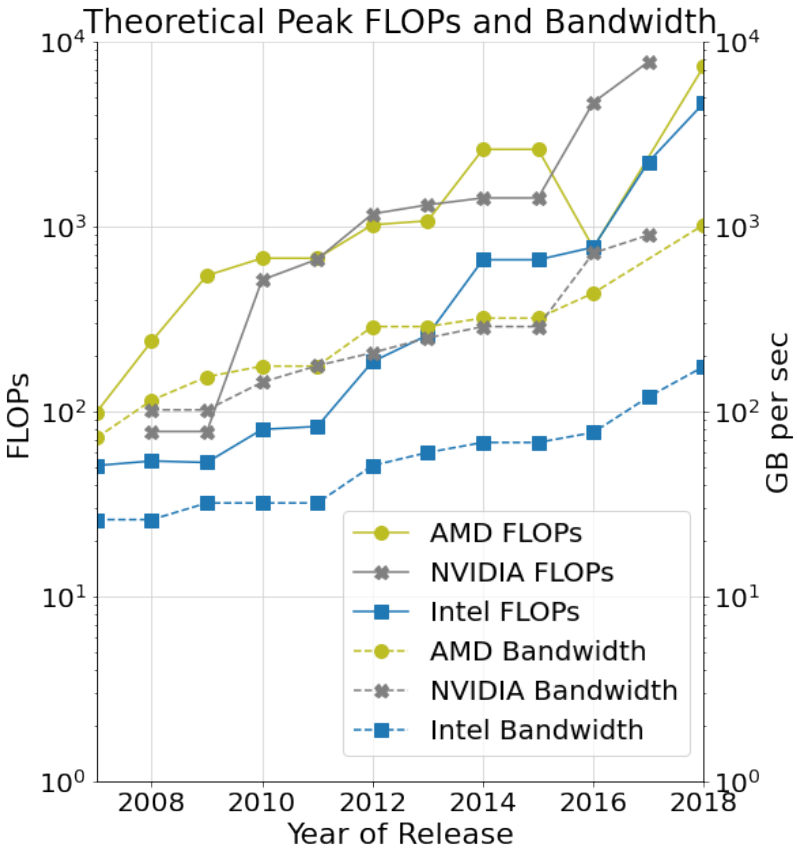


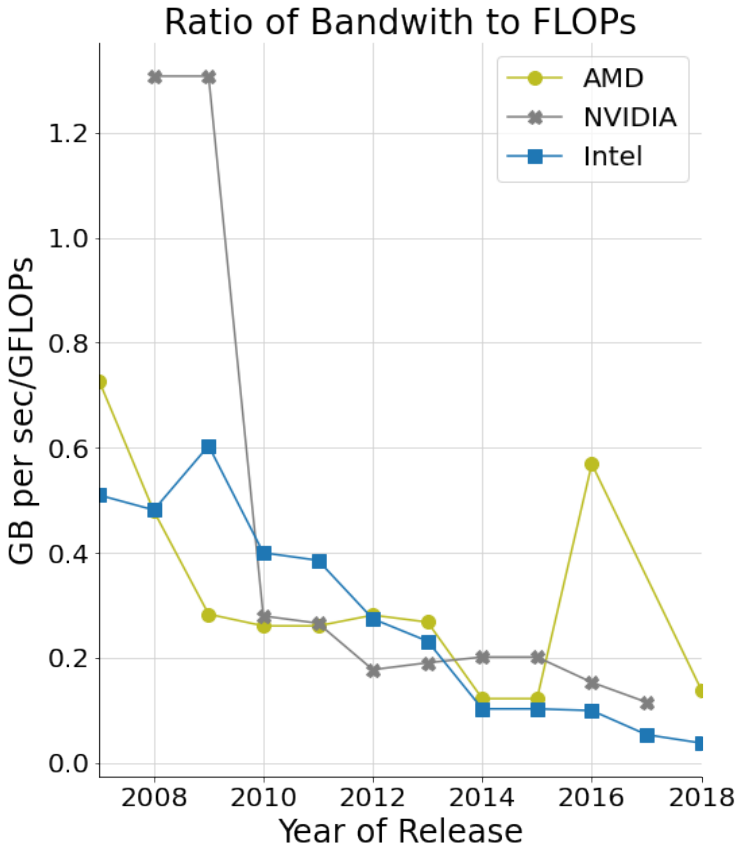


Modern hardware has lower memory bandwidth than FLOPs [4]

# Benefits of Matrix-Free

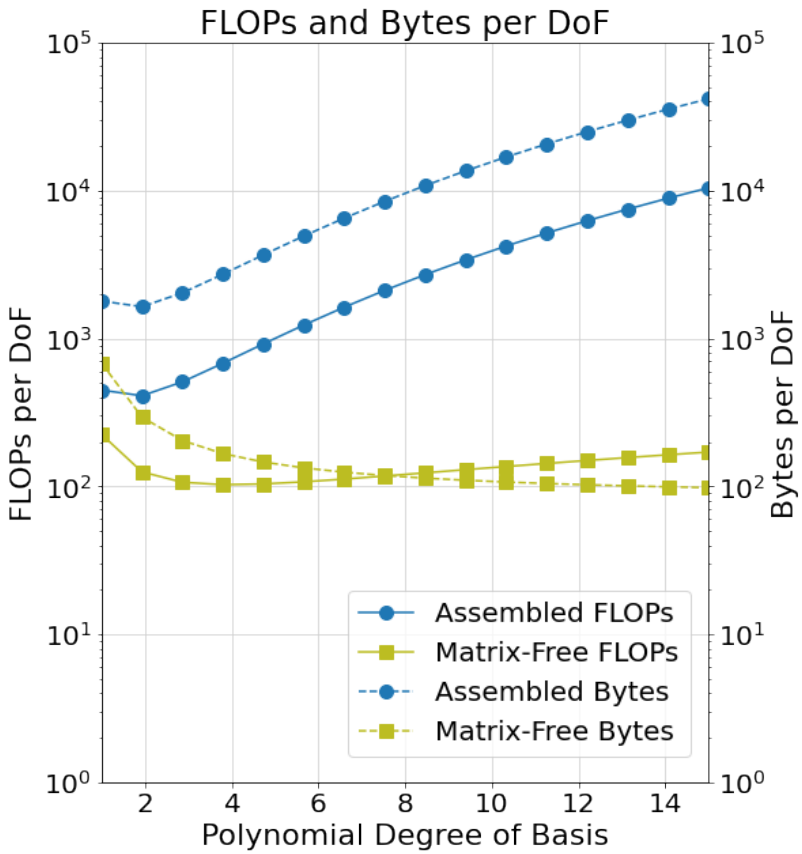


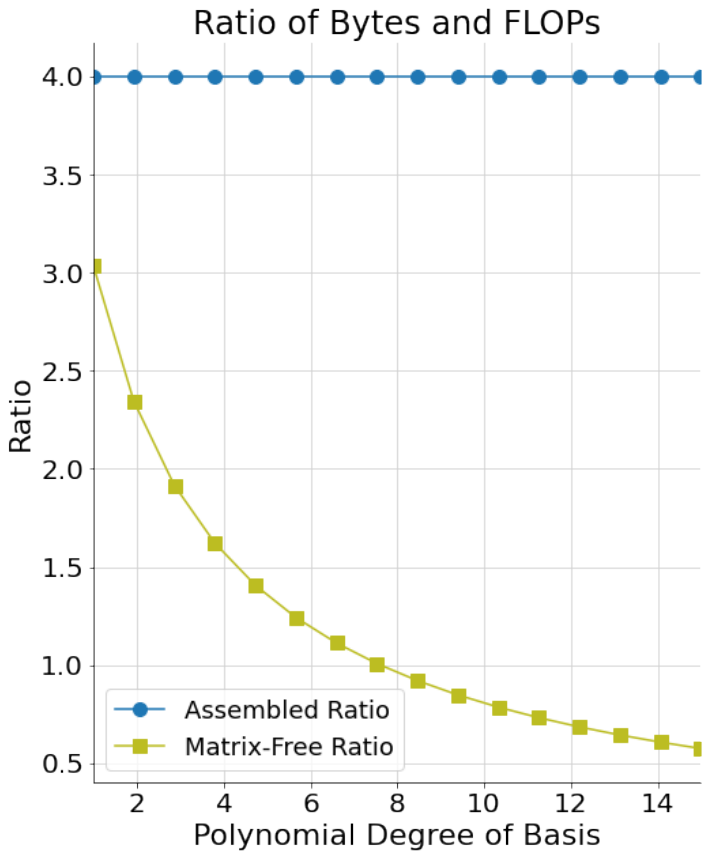


Requirements for matrix-vector product with sparse matrix vs matrix-free for screened Poisson $\nabla^2 u - \alpha^2 u = f$ in 3D

**Matrix-free representations using tensor product bases better match modern hardware limitations**

# Matrix-Free Representation

Weak form for an arbitrary second order PDE [2]:

$$\begin{gathered}\text{find } u \in V \text{ such that for all } v \in V \\ \langle v, u \rangle = \int_\Omega v \cdot f_0\left(u, \nabla u\right) + \nabla v : f_1\left(u, \nabla u\right) = 0\end{gathered} \tag{1}$$

- $\cdot$ - contraction over fields
- : - contraction over fields and spatial dimensions

# Matrix-Free Representation

Galerkin form for an arbitrary second order PDE:

$$\sum_e \mathcal{E}^T \left[ (\mathrm{N}^e)^T \mathrm{W}^e \Lambda \left( f_0 \left( u^e, \nabla u^e \right) \right) + \sum_{i=0}^{d-1} (\mathrm{D}_i^e)^T \mathrm{W}^e \Lambda \left( f_1 \left( u^e, \nabla u^e \right) \right) \right] = 0 \tag{2}$$

- $\mathcal{E}$ - element assembly/restriction operator
- $\mathrm{N}^e$ - interpolation to quadrature points
- $\mathrm{D}_i^e$ - derivatives at quadrature points
- $\mathrm{W}^e$ - quadrature weights
- $\Lambda$ - pointwise multiplication at quadrature points

# libCEED Representation

$$A = P^T G^T B^T D B G P$$

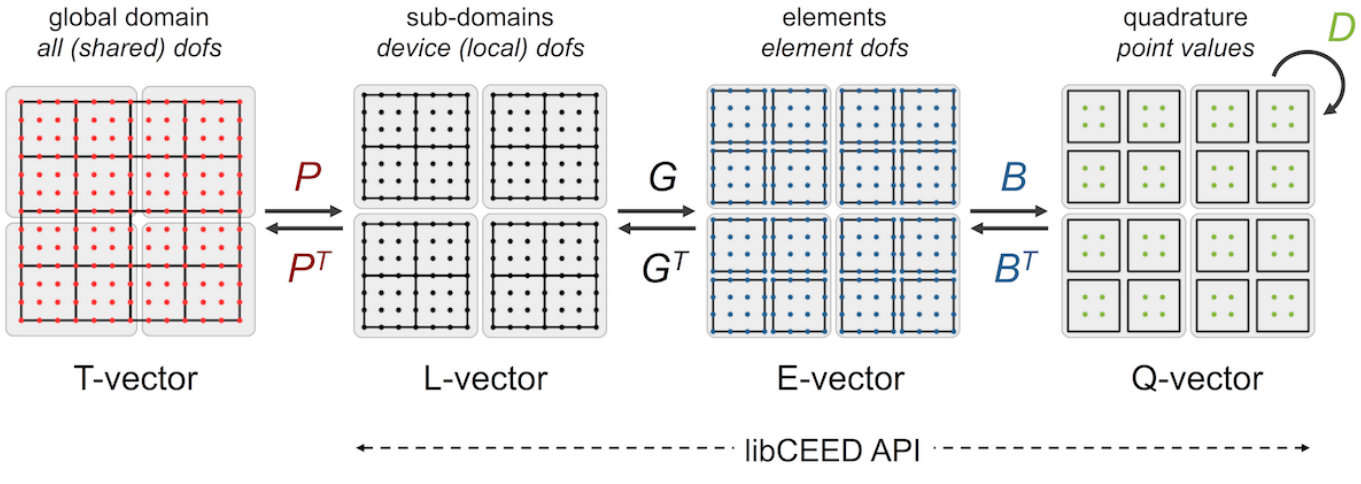


[1]

- P - parallel element assembly operator
- G - local element assembly operator
- B - basis action operator
- D - weak form and geometry at quadrature points

# LFA Background

Consider a scalar Toeplitz operator $L_h$ on the infinite 1D grid $G_h$

$$
\begin{aligned}
L_h &\hat{=} \left[s_\kappa\right]_h \left(\kappa \in V\right) \\
L_h w_h\left(x\right) &= \sum_{\kappa \in V} s_\kappa w_h\left(x + \kappa h\right)
\end{aligned}
\tag{3}
$$

where

- $V \subset \mathcal{Z}$ is an index set
- $s_k \in \mathcal{R}$ are constant coefficients
- $w_h\left(x\right)$ is a $l^2$ function on $G_h$

# LFA Background

If for all grid functions $\varphi(\theta, x)$

$$L_h \varphi(\theta, x) = \tilde{L}_h(\theta)\, \varphi(\theta, x) \tag{4}$$

then $\tilde{L}_h(\theta) = \sum_{\kappa \in V} s_\kappa e^{\imath \theta \kappa}$ is the **symbol** of $L_h$

Our function can be diagonalized by the standard Fourier modes

# LFA Background

For a $q \times q$ system of equations, the matrix symbol is given by

$$\mathsf{L}_h = \begin{bmatrix} L_h^{1,1} & \cdots & L_h^{1,q} \\ \vdots & \vdots & \vdots \\ L_h^{q,1} & \cdots & L_h^{q,q} \end{bmatrix} \quad \Rightarrow \quad \tilde{\mathsf{L}}_h = \begin{bmatrix} \tilde{L}_h^{1,1} & \cdots & \tilde{L}_h^{1,q} \\ \vdots & \vdots & \vdots \\ \tilde{L}_h^{q,1} & \cdots & \tilde{L}_h^{q,q} \end{bmatrix} \tag{5}$$

# LFA of High-Order FEM

For a scalar PDE operator on a single 1D finite element

$$\tilde{A}(\boldsymbol{\theta}) = Q^T \left( A^e \odot \left[ e^{\imath (x_j - x_i) \cdot \boldsymbol{\theta} / h} \right] \right) Q \tag{6}$$

where

$$A^e = B^T D B \tag{7}$$

$$Q = \begin{bmatrix} I \\ e_0 \end{bmatrix} = \begin{bmatrix} 1 & 0 & \cdots & 0 \\ 0 & 1 & \cdots & 0 \\ \vdots & \vdots & \vdots & \vdots \\ 0 & 0 & \cdots & 1 \\ 1 & 0 & \cdots & 0 \end{bmatrix} \tag{8}$$

# LFA of High-Order FEM

Symbol naturally extends to multiple components and higher dimensions

Multiple Components:

$$\mathsf{Q}_n = \mathsf{I}_n \otimes \mathsf{Q} \qquad (9)$$

Multiple Dimensions:

$$\mathsf{Q}_{nd} = \mathsf{Q} \otimes \mathsf{Q} \otimes \cdots \otimes \mathsf{Q} \qquad (10)$$

# Example: Scalar Poisson

$$\int \nabla v \nabla u = \int f v \tag{11}$$

- B - given by tensor H1 Lagrange basis
- D - given by quadrature weights and product

```
# mesh
dim = 1
mesh = Mesh1D(1.0)

# basis
p = 3
ncomp = 1
basis = TensorH1LagrangeBasis(p+1, p+1, ncomp, dim)

# weak form
function diffusionweakform(du::Array{Float64}, w::Array{Float64})
    return dv = du*w[1]
end
```

# Example: Scalar Poisson

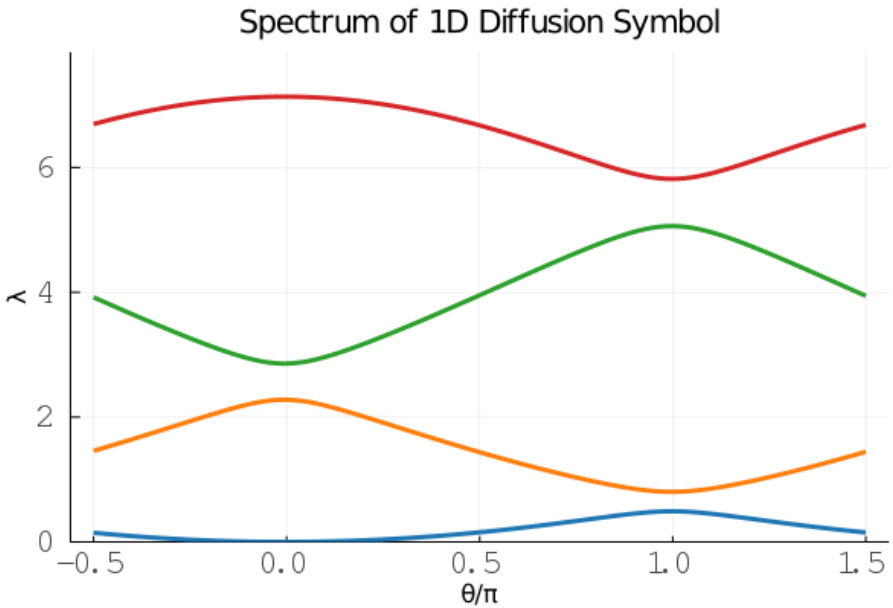


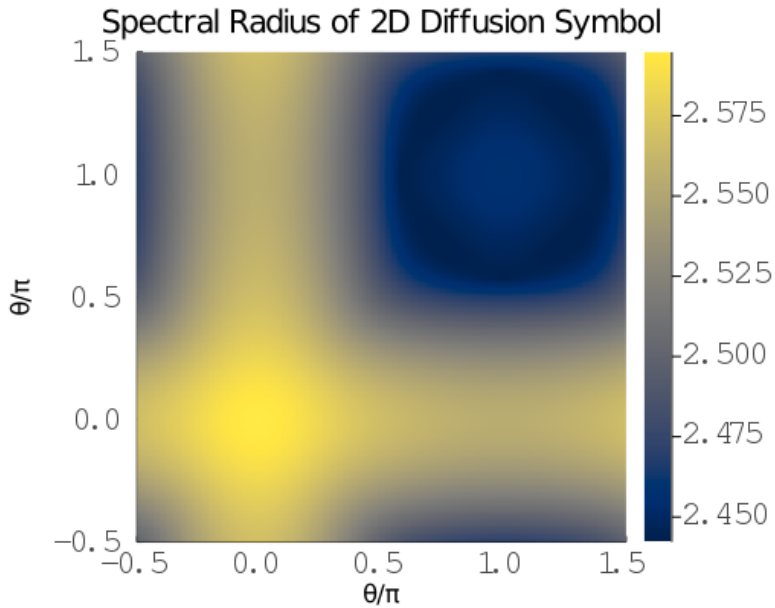


Scalar Poisson problem on quartic elements

low frequencies - $\theta \in T^{\text{low}} = [-\pi/2, \pi/2)^d$
high frequencies - $\theta \in T^{\text{high}} = [-\pi/2, 3\pi/2)^d \setminus T^{\text{low}}$

# LFA of High-Order Smoothers

Error propagation operator for smoothers given by

$$\mathrm{S} = \mathrm{I} - \mathrm{M}^{-1} A \tag{12}$$

with a symbol given by

$$\tilde{\mathrm{S}}\left(\omega, \boldsymbol{\theta}\right) = \mathrm{I} - \tilde{\mathrm{M}}^{-1}\left(\omega, \boldsymbol{\theta}\right) \tilde{A}\left(\boldsymbol{\theta}\right) \tag{13}$$

# Jacobi Smoothing

Jacobi smoothing given by

$$\mathrm{M}^{-1} = \omega \ \mathrm{diag}\left(A\right)^{-1} \tag{14}$$

with an error symbol given by

$$\tilde{\mathrm{S}}\left(\omega, \boldsymbol{\theta}\right) = \mathrm{I} - \omega \ \left(\mathrm{Q}^{T} \, \mathrm{diag}\left(A^{e}\right) \mathrm{Q}\right)^{-1} \tilde{A}\left(\boldsymbol{\theta}\right) \tag{15}$$

# Example: Jacobi Smoothing

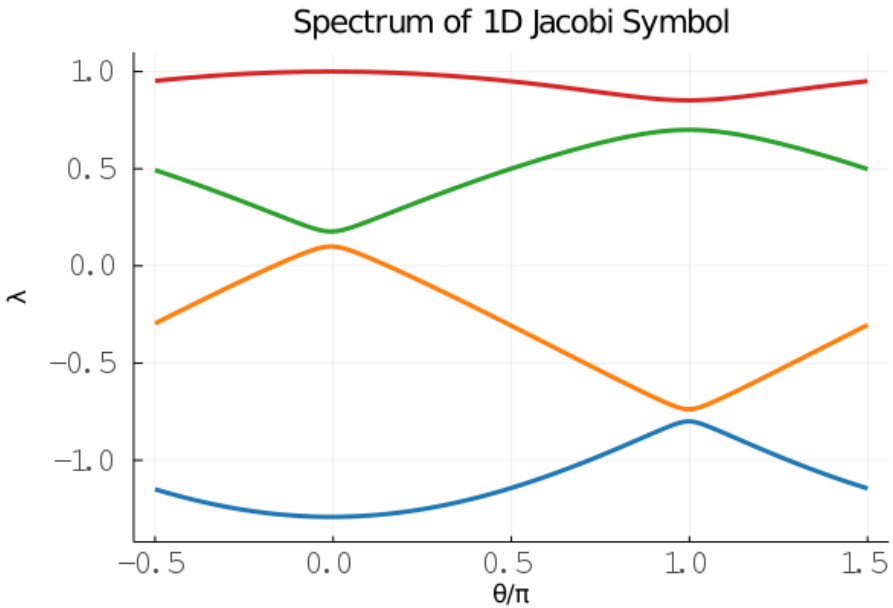


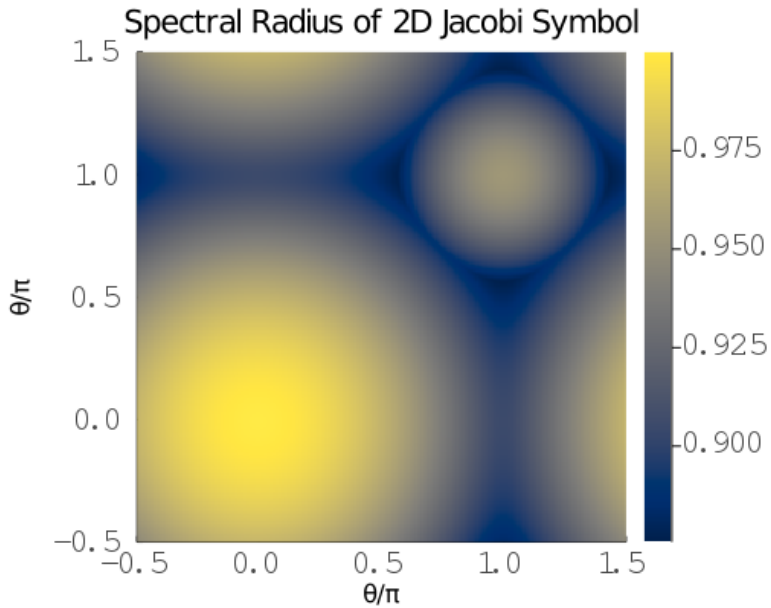


Jacobi smoothing with $\omega = 1.0$ on quartic elements

low frequencies - $\theta \in T^{\text{low}} = [-\pi/2, \pi/2)^d$
high frequencies - $\theta \in T^{\text{high}} = [-\pi/2, 3\pi/2)^d \setminus T^{\text{low}}$

# Chebyshev Smoother

Error in *kth* order Chebyshev smoothing is given by

$$\begin{aligned} \mathsf{E}_0 &= \mathsf{I} \\ \mathsf{E}_1 &= \mathsf{I} - \tfrac{1}{\alpha} \left(\operatorname{diag} \mathsf{A}\right)^{-1} \mathsf{A} \\ \mathsf{E}_k &= \left( \left(\operatorname{diag} \mathsf{A}\right)^{-1} \mathsf{A}\mathsf{E}_{k-1} - \alpha \mathsf{E}_{k-1} - \beta_{k-2} \mathsf{E}_{k-2} \right) / \gamma_{k-1} \end{aligned} \tag{16}$$

for an operator with a spectrum on the interval $[\alpha - c, \alpha + c]$ where

$$\begin{aligned} \beta_0 &= -\frac{c^2}{2\alpha} & \gamma_0 &= -\alpha \\ \beta_k &= \frac{c}{2} \frac{T_k(\eta)}{T_{k+1}(\eta)} = \left(\frac{c}{2}\right)^2 \frac{1}{\gamma_k} & \gamma_k &= \frac{c}{2} \frac{T_{k+1}(\eta)}{T_k(\eta)} = -\left(\alpha + \beta_{k-1}\right). \end{aligned} \tag{17}$$

# Chebyshev Smoother

The error symbol of $k$th order Chebyshev smoother is given by

$$\begin{aligned}
\tilde{\mathsf{E}}_0(\boldsymbol{\theta}) &= \mathsf{I} \\
\tilde{\mathsf{E}}_1(\boldsymbol{\theta}) &= \mathsf{I} - \tfrac{1}{\alpha}\tilde{\mathsf{A}}_J\tilde{\mathsf{A}}(\boldsymbol{\theta}) \\
\tilde{\mathsf{E}}_k(\boldsymbol{\theta}) &= \left(\tilde{\mathsf{A}}_J\tilde{\mathsf{A}}(\boldsymbol{\theta})\,\tilde{\mathsf{E}}_{k-1}(\boldsymbol{\theta}) - \alpha\tilde{\mathsf{E}}_{k-1}(\boldsymbol{\theta}) - \beta_{k-2}\tilde{\mathsf{E}}_{k-2}(\boldsymbol{\theta})\right)/\gamma_{k-1}
\end{aligned} \tag{18}$$

with $\tilde{A}_J$ being the symbol of the Jacobi preconditioner

# Example: Chebyshev Smoothing

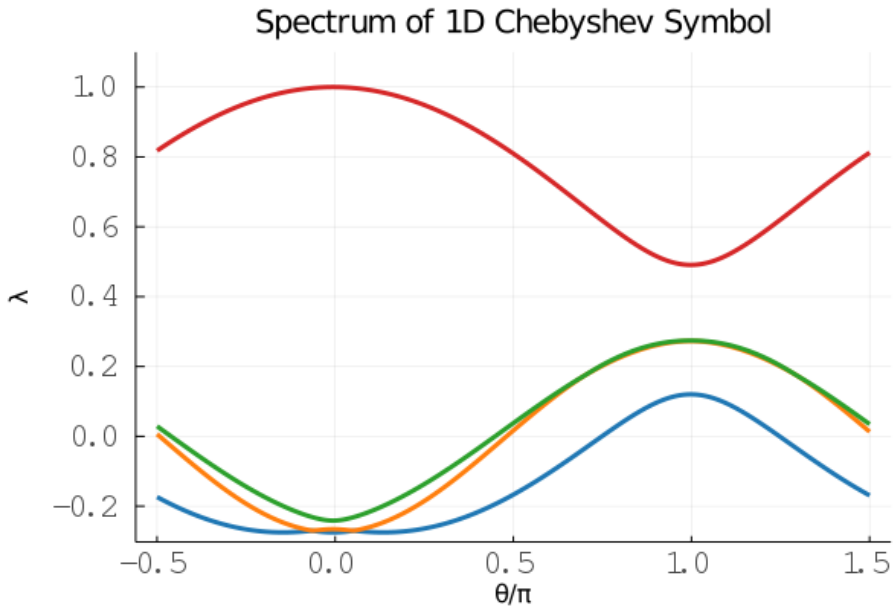


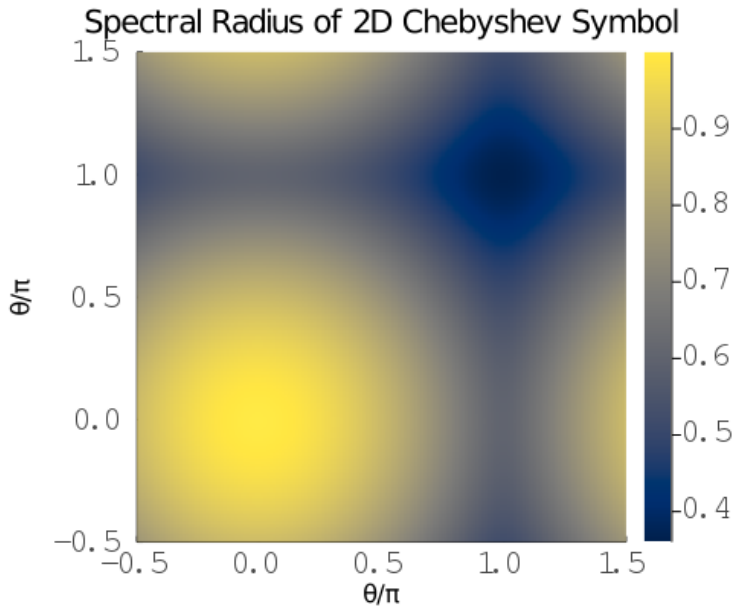


Third order Chebyshev smoothing quartic elements

$$\text{low frequencies - } \theta \in T^{\text{low}} = [-\pi/2, \pi/2)^d$$
$$\text{high frequencies - } \theta \in T^{\text{high}} = [-\pi/2, 3\pi/2)^d \setminus T^{\text{low}}$$

# Two-Grid Multigrid Error

Multigrid methods target the low frequency error

$$E_{2MG} = S_f \left( I - P_{ctof} A_c^{-1} R_{ftoc} A_f \right) S_f \tag{19}$$

- $A_f$ - fine grid PDE operator
- $A_c^{-1}$ - coarse grid solve (low frequency error)
- $S_f$ - fine grid smoother (high frequency error)
- $P_{ctof}$ - coarse to fine grid prolongation operator
- $R_{ftoc}$ - fine to coarse grid restriction operator

Grid transfer operators and coarse representation differentiate h-multigrid and p-multigrid

# Two-Grid Multigrid Error

The definition of the symbol follows naturally

$$\tilde{E}_{2MG}(\boldsymbol{\theta}) = \tilde{S}_f(\boldsymbol{\theta}, \omega)\left(I - \tilde{P}_{ctof}(\boldsymbol{\theta})\left(\tilde{A}_c(\boldsymbol{\theta})\right)^{-1}\tilde{R}_{ftoc}(\boldsymbol{\theta})\,\tilde{A}_f(\boldsymbol{\theta})\right)\tilde{S}_f(\boldsymbol{\theta}, \omega) \tag{20}$$

- $A_f$ - fine grid PDE operator
- $A_c^{-1}$ - coarse grid solve (low frequency error)
- $S_f$ - fine grid smoother (high frequency error)
- $P_{ctof}$ - coarse to fine grid prolongation operator
- $R_{ftoc}$ - fine to coarse grid restriction operator

# P-Multigrid Transfer Operators

P-multigrid prolongation can be represented as an interpolation from the coarse to fine grid

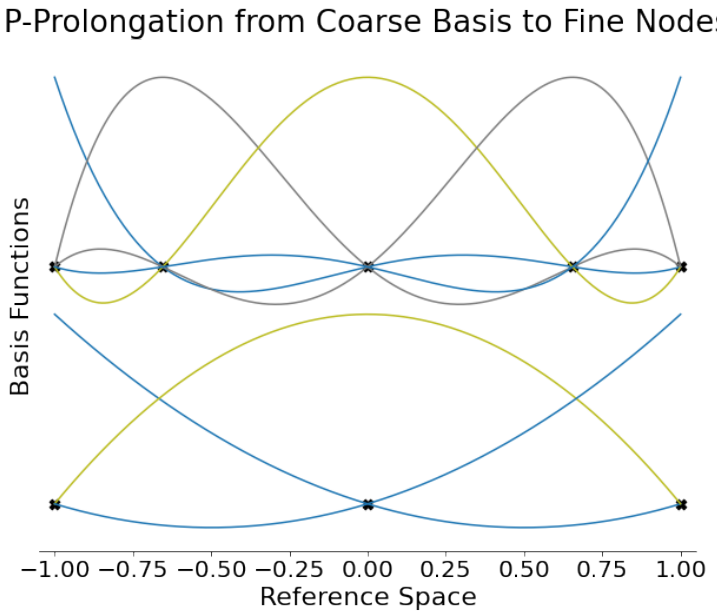


$$\mathsf{P}_{\text{ctof}} = \mathsf{P}_f^T \mathsf{G}_f^T \mathsf{P}_e \mathsf{G}_c \mathsf{P}_c$$
$$\mathsf{P}_e = \mathsf{I}\mathsf{D}_{\text{scale}} \mathsf{B}_{\text{ctof}} \tag{21}$$

D scales for node multiplicity

# Example: P-Multigrid

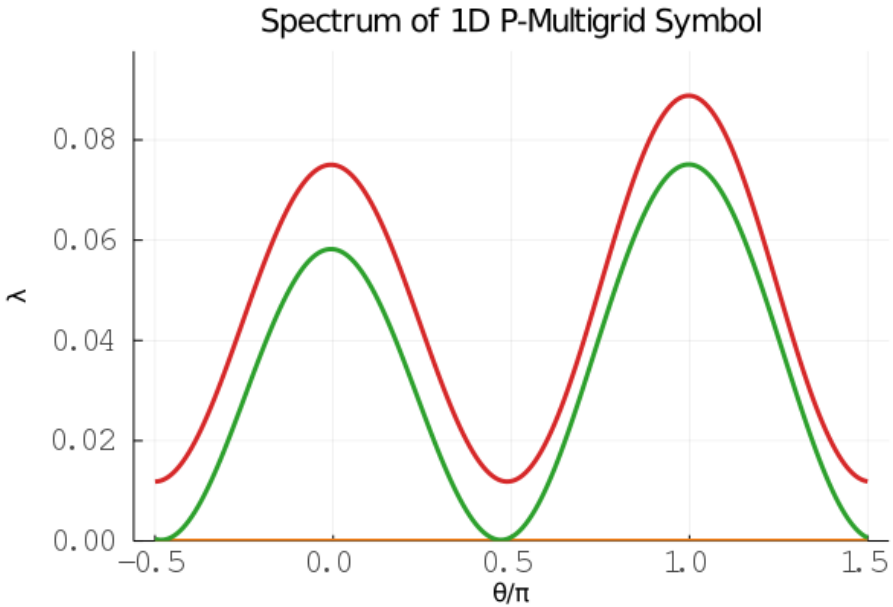


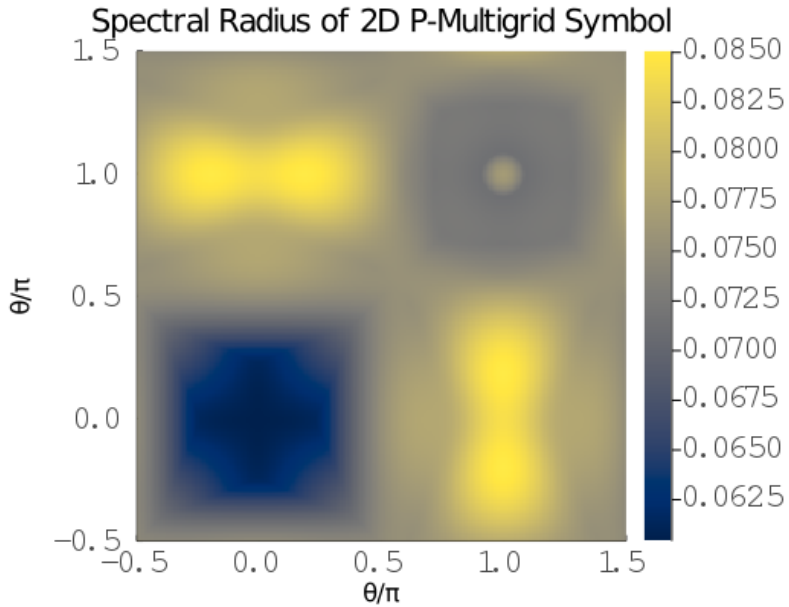


p-multigrid with third order Chebyshev on quadratic to linear elements

$$\text{low frequencies - } \theta \in T^{\text{low}} = [-\pi/2, \pi/2)^d$$
$$\text{high frequencies - } \theta \in T^{\text{high}} = [-\pi/2, 3\pi/2)^d \setminus T^{\text{low}}$$

# Validation: P-Multigrid

| $p_{\text{fine}}$ to $p_{\text{coarse}}$ | LFA | libCEED |
|---|---|---|
| $p = 2$ to $p = 1$ | 0.312 | 0.301 |
| $p = 4$ to $p = 2$ | 1.436 | 1.402 |
| $p = 4$ to $p = 1$ | 1.436 | 1.401 |
| $p = 8$ to $p = 4$ | 1.989 | 1.885 |
| $p = 8$ to $p = 2$ | 1.989 | 1.874 |
| $p = 8$ to $p = 1$ | 1.989 | 1.875 |

LFA and experimental two-grid convergence factors with Jacobi smoothing for 3D Laplacian with $\omega = 1.0$

3D manufactured solution on the domain $[-3, 3]^3$ with Dirichlet boundaries:

$$f(x, y, z) = xyz \sin(\pi x) \sin(\pi(1.23 + 0.5y)) \sin(\pi(2.34 + 0.25z)) \quad (22)$$

# Validation: P-Multigrid

| $p_{\text{fine}}$ to $p_{\text{coarse}}$ | $k=2$ | | $k=3$ | | $k=4$ | |
|---|---|---|---|---|---|---|
| | LFA | libCEED | LFA | libCEED | LFA | libCEED |
| $p=2$ to $p=1$ | 0.253 | 0.222 | 0.076 | 0.058 | 0.041 | 0.033 |
| $p=4$ to $p=2$ | 0.277 | 0.251 | 0.111 | 0.097 | 0.062 | 0.050 |
| $p=4$ to $p=1$ | 0.601 | 0.587 | 0.416 | 0.398 | 0.295 | 0.276 |
| $p=8$ to $p=4$ | 0.398 | 0.391 | 0.197 | 0.195 | 0.121 | 0.110 |
| $p=8$ to $p=2$ | 0.748 | 0.743 | 0.611 | 0.603 | 0.506 | 0.469 |
| $p=8$ to $p=1$ | 0.920 | 0.914 | 0.871 | 0.861 | 0.827 | 0.814 |

LFA and experimental two-grid convergence factors with Chebyshev smoothing for 3D Laplacian

# H-Multigrid Transfer Operators

H-multigrid prolongation can be represented as an interpolation from the coarse grid to fine grid macro-elements

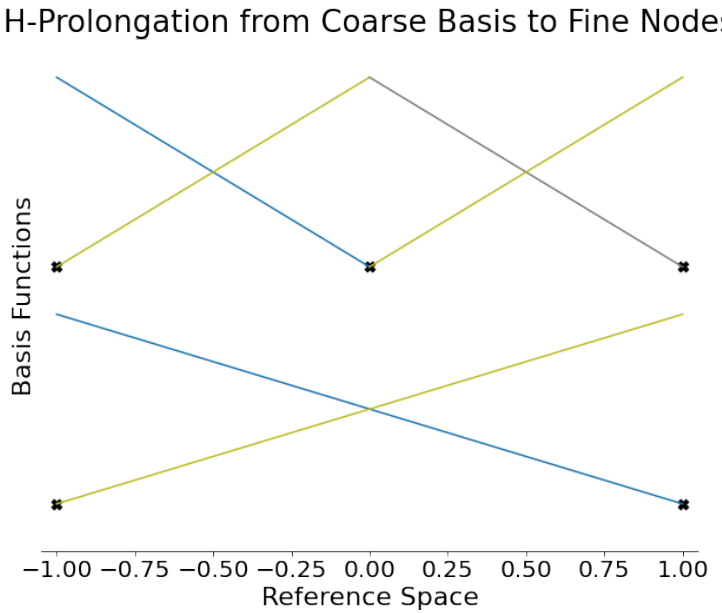


$$\begin{aligned} \mathsf{P}_{\text{ctof}} &= \mathsf{P}_f^T \mathsf{G}_f^T \mathsf{P}_e \mathsf{G}_c \mathsf{P}_c \\ \mathsf{P}_e &= \mathsf{ID}_{\text{scale}} \mathsf{B}_{\text{ctof}} \end{aligned} \tag{23}$$

D scales for node multiplicity

# Example: H-Multigrid

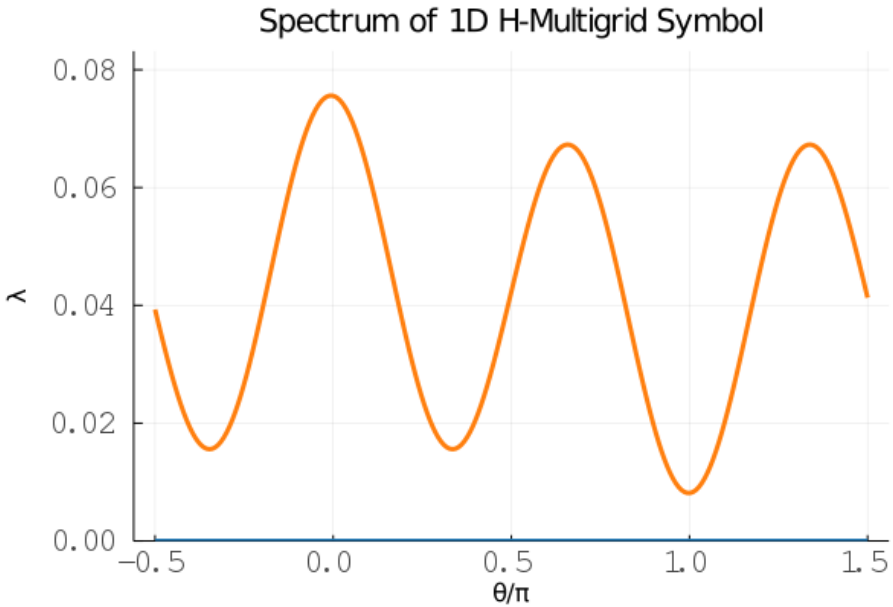


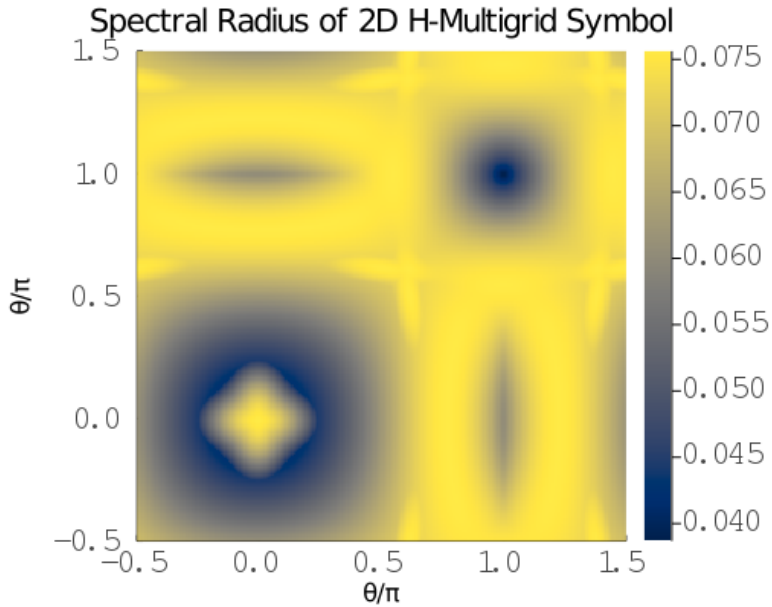


h-multigrid with third order Chebyshev on linear elements

$$\text{low frequencies - } \theta \in T^{\text{low}} = [-\pi/2, \pi/2)^d$$
$$\text{high frequencies - } \theta \in T^{\text{high}} = [-\pi/2, 3\pi/2)^d \setminus T^{\text{low}}$$

# Validation: P-Multigrid

| $p, d$ | $\nu = (0,1)$ | | $\nu = (1,1)$ | | $\nu = (2,2)$ | |
|---|---|---|---|---|---|---|
| | $\rho$ | $\omega$ | $\rho$ | $\omega$ | $\rho$ | $\omega$ |
| $p = 2, d = 1$ | 0.821 | 1.000 | 0.821 | 1.000 | 1.279 | 1.000 |
| $p = 2, d = 1$ | 0.526 | 0.838 | 0.495 | 0.838 | 0.302 | 0.838 |
| $p = 2, d = 1$ | 0.291 | 0.709 | 0.249 | 0.709 | 0.064 | 0.709 |
| $p = 3, d = 1$ | 0.491 | 0.650 | 0.337 | 0.650 | 0.131 | 0.650 |
| $p = 4, d = 1$ | 0.608 | 0.640 | 0.559 | 0.640 | 0.331 | 0.640 |
| $p = 2, d = 2$ | 0.452 | 1.000 | 0.288 | 1.000 | 0.091 | 1.000 |

Two-grid convergence factor and Jacobi smoothing parameter for high-order h-multigrid

Results agree with previous work [3]

# Big Picture

- High-order matrix-free representations of PDEs are better suited to modern hardware than sparse matrices
- High-order matrix-free representations require preconditioned iterative solvers
- Local Fourier Analysis (LFA) provides sharp convergence estimates for these preconditioners
- We develop LFA of p-multigrid and Balancing Domain Decomposition by Constraints (BDDC) on high-order element subdomains
- Further, we investigate LFA of p-multigrid with a BDDC smoother

# Big Picture

- High-order matrix-free representations of PDEs are better suited to modern hardware than sparse matrices
- High-order matrix-free representations require preconditioned iterative solvers
- Local Fourier Analysis (LFA) provides sharp convergence estimates for these preconditioners
- We develop LFA of p-multigrid and Balancing Domain Decomposition by Constraints (BDDC) on high-order element subdomains
- Further, we investigate LFA of p-multigrid with a BDDC smoother

# Local Fourier Analysis of Domain Decomposition and Multigrid Methods for High-Order Matrix-Free Finite Elements

Jeremy L Thompson

University of Colorado Boulder

*jeremy@jeremylt.org*

July 8, 2021


Ahmad Abdelfattah, Valeria Barra, Natalie Beams, Jed Brown, Jean-Sylvain Camier, Veselin Dobrev, Yohann Dudouit, Leila Ghaffari, Tzanio Kolev, David Medina, Thilina Rathnayake, Jeremy L Thompson, and Stanimire Tomov.
libCEED User Manual, September 2020.


Jed Brown.
Efficient nonlinear solvers for nodal high-order finite elements in 3D.
*Journal of Scientific Computing*, 45(1-3):48–63, 2010.


Yunhui He and Scott MacLachlan.
Two-level fourier analysis of multigrid for higher-order finite-element discretizations of the laplacian.
*Numerical Linear Algebra with Applications*, 27(3):e2285, 2020.


Karl Rupp.
CPU-GPU-MIC comparision charts, 2020.

# Local Fourier Analysis of Domain Decomposition and Multigrid Methods for High-Order Matrix-Free Finite Elements

Jeremy L Thompson

University of Colorado Boulder

*jeremy@jeremylt.org*

July 8, 2021